OPEN ACCESS Freely available online

PLOS ONE

Proper Interpretation of Dissolved Nitrous Oxide Isotopes, Production Pathways, and Emissions Requires a Modelling Approach

Simon J. Thuss¤, Jason J. Venkiteswaran*, Sherry L. Schiff

Department of Earth and Environmental Sciences, University of Waterloo, Waterloo, Ontario, Canada

Abstract

Stable isotopes (δ^{15}N and δ^{18}O) of the greenhouse gas N_2O provide information about the sources and processes leading to N_2O production and emission from aquatic ecosystems to the atmosphere. In turn, this describes the fate of nitrogen in the aquatic environment since N_2O is an obligate intermediate of denitrification and can be a by-product of nitrification. However, due to exchange with the atmosphere, the δ values at typical concentrations in aquatic ecosystems differ significantly from both the source of N_2O and the N_2O emitted to the atmosphere. A dynamic model, SIDNO, was developed to explore the relationship between the isotopic ratios of N_2O, N_2O source, and the emitted N_2O. If the N_2O production rate or isotopic ratios vary, then the N_2O concentration and isotopic ratios may vary or be constant, not necessarily concomitantly, depending on the synchronicity of production rate and source isotopic ratios. Thus *prima facie* interpretation of patterns in dissolved N_2O concentrations and isotopic ratios is difficult. The dynamic model may be used to correctly interpret diel field data and allows for the estimation of the gas exchange coefficient, N_2O production rate, and the production-weighted δ values of the N_2O source in aquatic ecosystems. Combining field data with these modelling efforts allows this critical piece of nitrogen cycling and N_2O flux to the atmosphere to be assessed.

Citation: Thuss SJ, Venkiteswaran JJ, Schiff SL (2014) Proper Interpretation of Dissolved Nitrous Oxide Isotopes, Production Pathways, and Emissions Requires a Modelling Approach. PLoS ONE 9(3): e90641. doi:10.1371/journal.pone.0090641

Editor: David William Pond, Scottish Association for Marine Science, United Kingdom

Received July 15, 2013; **Accepted** February 3, 2014; **Published** March 7, 2014

Funding: Funding was provided by a Natural Sciences and Engineering Research Council (NSERC) and BIOCAP grant 336807-06 (SLS), an NSERC scholarship (SJT), and Environment Canada's Science Horizons Youth Internship Program. The funders had no role in study design, data collection and analysis, decision to publish, or preparation of the manuscript.

Competing Interests: BIOCAP, closed in 2008, was a commercial funder. This does not alter our adherence to all the PLOS ONE policies on sharing data and materials.

* E-mail: jjvenkit@uwaterloo.ca

¤ Current address: Golder Associates, London, ON, Canada

Introduction

Nitrous oxide (N_2O) is a powerful greenhouse gas, 298 times more potent than CO_2 over a 100-year time line [1]. Atmospheric N_2O concentrations have been increasing at a rate of 0.25%/year over the last 150 years [2]. Consequently, the global N_2O budget has been the subject of intensive research efforts over the past few decades. N_2O is produced through multiple microbial pathways: hydroxylamine oxidation during nitrification and as an obligate intermediate during denitrification and nitrifier–denitrification. Because these pathways of N_2O production have different stable isotopic enrichment factors, isotopic analysis of N_2O can potentially distinguish N_2O produced through different pathways or from different sources [3]. Identifying N_2O sources will provide insights on the fate of N at the ecosystem-scale (e.g., [4–6]). The isotopic ratios of N_2O produced in soil environments (e.g., [7–11]), and in aquatic environments (e.g., [12–18]) have been measured to some extent. Although N_2O production in rivers and estuaries is a significant portion of the global N_2O budget (approximately 1.5 TgN/year, [19]), few studies report isotopic data for rivers [5,20,21].

In ice-free aquatic ecosystems, the δ^{15}N and δ^{18}O of dissolved N_2O is affected by gas exchange with the atmosphere. As a result, the isotopic ratios of dissolved N_2O are not equal to those of the N_2O produced within the aquatic ecosystem and continue to change as atmospheric exchange (both ingassing and outgassing) occurs. In addition, isotopic fractionation during influx and efflux causes the isotopic ratios of N_2O flux emitted to the atmosphere to be different than that of the dissolved N_2O [22]. Thus, the simple method of calculating the instantaneous isotopic ratios of the N_2O flux by taking measured dissolved isotopic ratios, adding an equilibrium isotope fractionation, and applying them to measured flux rates is inappropriate. Adjustments of measured isotopic ratios are necessary to understand the isotopic ratios of both produced and emitted N_2O.

In this paper, we present a dynamic model of the stable isotopic composition of both the dissolved and emitted N_2O in aqueous systems. We apply this model to two different measured diel patterns of the isotopic ratios of N_2O in an aquatic ecosystem. We use the model to elucidate the relationship between the isotopic ratios of source, dissolved, and emitted N_2O, to allow for improved interpretation of dissolved N_2O isotope data. Ultimately, a process-based understanding on N cycling with aquatic ecosystems may be developed based on interpretation of N cycling processes.

Materials and Methods

Stable Isotopes of N_2O

N_2O is an asymmetric molecule: the most abundant isotopologues of N_2O are [$^{14}N^{14}N^{16}O$], [$^{15}N^{14}N^{16}N$], [$^{14}N^{15}N^{16}O$] and [$^{14}N^{14}N^{18}O$]. The isotopic ratios, ^{15}N: ^{14}N and ^{18}O: ^{16}O, are:

$$^{15}R = \frac{[^{15}N^{14}N^{16}O] + [^{14}N^{15}N^{16}O]}{2[^{14}N^{14}N^{16}O]} = \frac{[^{15}N_2O]}{[^{14}N_2O]} \quad (1)$$

$$^{18}R = \frac{[^{14}N^{14}N^{18}O]}{[^{14}N^{14}N^{16}O]} = \frac{[N_2{}^{18}O]}{[N_2{}^{16}O]} \quad (2)$$

where [$^{14}N^{14}N^{16}O$], [$^{15}N^{14}N^{16}O$], [$^{14}N^{15}N^{16}O$] and [$^{14}N^{14}N^{18}O$] represent the concentrations of the various N_2O isotopologues. Note that 15R is the bulk ^{15}N: ^{14}N ratio and represents an average ratio of the two ^{15}N isotopomers and isotopic ratios are reported as $\delta^{15}N$ relative to air and $\delta^{18}O$ relative to VSMOW. Although the isotopic ratio of the ^{15}N isotopomers can be measured (e.g., [23–25]), the gas exchange fractionation factors are not affected by the intramolecular distribution of ^{15}N [22]. Many laboratories cannot measure the intramolecular distribution of ^{15}N and analysis of the bulk ^{15}N: ^{14}N ratio of N_2O is more common [26]. Here, we confine our analysis to bulk ^{15}N: ^{14}N ratios and use $^{15}N_2O$ to represent the average abundance of the two ^{15}N isotopomers. The same approach could easily be extended to consider each isotopologue separately.

Dynamic Isotope Model for Dissolved N_2O

A simple three box model (SIDNO, Stable Isotopes of Dissolved Nitrous Oxide) was created using Stella modelling software (version 9.1.4, http://www.iseesystems.com) in order to study the relationships between the isotopic ratios of source, dissolved and emitted N_2O (model file is available at https://github.com/jjvenky/SIDNO and by contacting the corresponding author). This model is an adaptation of the isotopic gas exchange portion of the PoRGy model [27], which successfully modelled diel isotopic ratios of O_2 resulting from photosynthesis, respiration, and gas exchange in aquatic ecosystems. One key difference is photosynthetically produced O_2 in PoRGy has a $\delta^{18}O$ value fixed by the H_2O molecules, whereas SIDNO has N_2O production $\delta^{15}N$ and $\delta^{18}O$ values that can vary independently of each other and of N_2O production rate in order to simulate variability in nitrification and denitrification.

One box in SIDNO is used for the total mass of dissolved N_2O and two additional boxes for the dissolved masses of the two heavy isotopologues ($^{15}N_2O$ and $N_2{}^{18}O$). The boxes are open to the atmosphere for gas exchange, are depth agnostic, and each box can gain N_2O via a production term; there is no N_2O consumption term since the δ values of N_2O are largely controlled by the production pathways [28,29] though certain waters can exhibit significant N_2O reduction to N_2 [30,31]. The masses and magnitude of the flows of $^{15}N_2O$ and $N_2{}^{18}O$ relative to bulk N_2O are used to calculate the isotopic composition of source, dissolved, and emitted N_2O. Although isotopic ratios are used in the model, we discuss δ values that are common for reporting isotopic ratios. N_2O production rate and its δ values are user-defined and can be adjusted for diel patterns in N_2O production that may be caused by variable O_2 levels [32–37].

Stable Isotope Dynamics of Gas Exchange

The δ values of the net gas exchange flux are controlled by the kinetic fractionation factors for evasion ($\alpha_{ev} = R_{evaded}/R_{dissolved}$, 0.9993 for $\delta^{15}N$ and 0.9981 for $\delta^{18}O$) and invasion ($\alpha_{in} = R_{invaded}/R_{gas}$, 1.0000 for $\delta^{15}N$ and 0.9992 for $\delta^{18}O$) [22]. These two α values are related to the equilibrium fractionation factor: $\alpha_{eq} = R_{gas}/R_{dissolved} = \alpha_{ev}/\alpha_{in}$ (0.99925 for $\delta^{15}N$ and 0.99894 for $\delta^{18}O$) and are independent of temperature over the range of 0°C to 44.5°C [22].

The δ values of tropospheric N_2O are 6.72 ‰ ± 0.12‰ for $\delta^{15}N$ and 44.62‰ ± 0.21‰ for $\delta^{18}O$ [38]. Therefore, at equilibrium, dissolved N_2O has dissolved δ values slightly greater than these at 7.48‰ and 45.73‰, respectively.

In the model, net N_2O flux between the atmosphere and dissolved phase was calculated using the thin boundary layer approach as:

$$Flux = k\left(p_{N_2O} \times k_H - [N_2O]_{dissolved}\right) \quad (3)$$

where the N_2O flux is calculated in mol/m^2/h, k is the user-modifiable gas exchange coefficient (m/h), is the partial pressure of tropospheric N_2O (assumed to be 320 ppbv from data provided by the ALE GAGE AGAGE investigators, [39,40]), k_H is the Henry constant for N_2O (mol/atm-m^3), and $[N_2O]_{dissolved}$ is the dissolved concentration of N_2O (mol/m^3). k_H is a function of water temperature [41]:

$$k_H = 0.025e^{-2600\left(\frac{1}{T} - \frac{1}{298.15}\right)} \quad (4)$$

where T is temperature in kelvins.

Gas exchange is a two-way process. The net N_2O flux rate (the difference between the invasion and evasion rates) depends on the dissolved N_2O concentration. When a solution is at equilibrium with the atmosphere, the invasion and evasion rates will be equal, and the net flux will be zero.

As with the bulk N_2O flux, the flux of the heavy isotopologues ($^{15}N_2O$ and $N_2{}^{18}O$) can be calculated by including the kinetic fractionation factors for N_2O (adapted from [27]):

$$Flux\,{}^{15}N_2O = k\left(\alpha_{in}^{15} \times p_{{}^{15}N_2O} \times k_H - \alpha_{ev}^{15}[{}^{15}N_2O]_{dissolved}\right) \quad (5)$$

$$Flux\,N_2{}^{18}O = k\left(\alpha_{in}^{18} \times p_{N_2{}^{18}O} \times k_H - \alpha_{ev}^{18}[N_2{}^{18}O]_{dissolved}\right) \quad (6)$$

where $p_{{}^{15}N_2O}$ and $p_{N_2{}^{18}O}$ are the partial pressures of $^{15}N_2O$ and $N_2{}^{18}O$.

Results

Test of Model Performance

To test the ability of SIDNO to reproduce observed isotopic data, input parameters (N_2O production rate, N_2O δ values, and k) were set to replicate a series of experiments designed to derive fractionation factors for N_2O gas exchange [22]. In these experiments, degassed water was exposed to N_2O gas of known isotopic ratios in a sealed container to varying degrees of saturation.

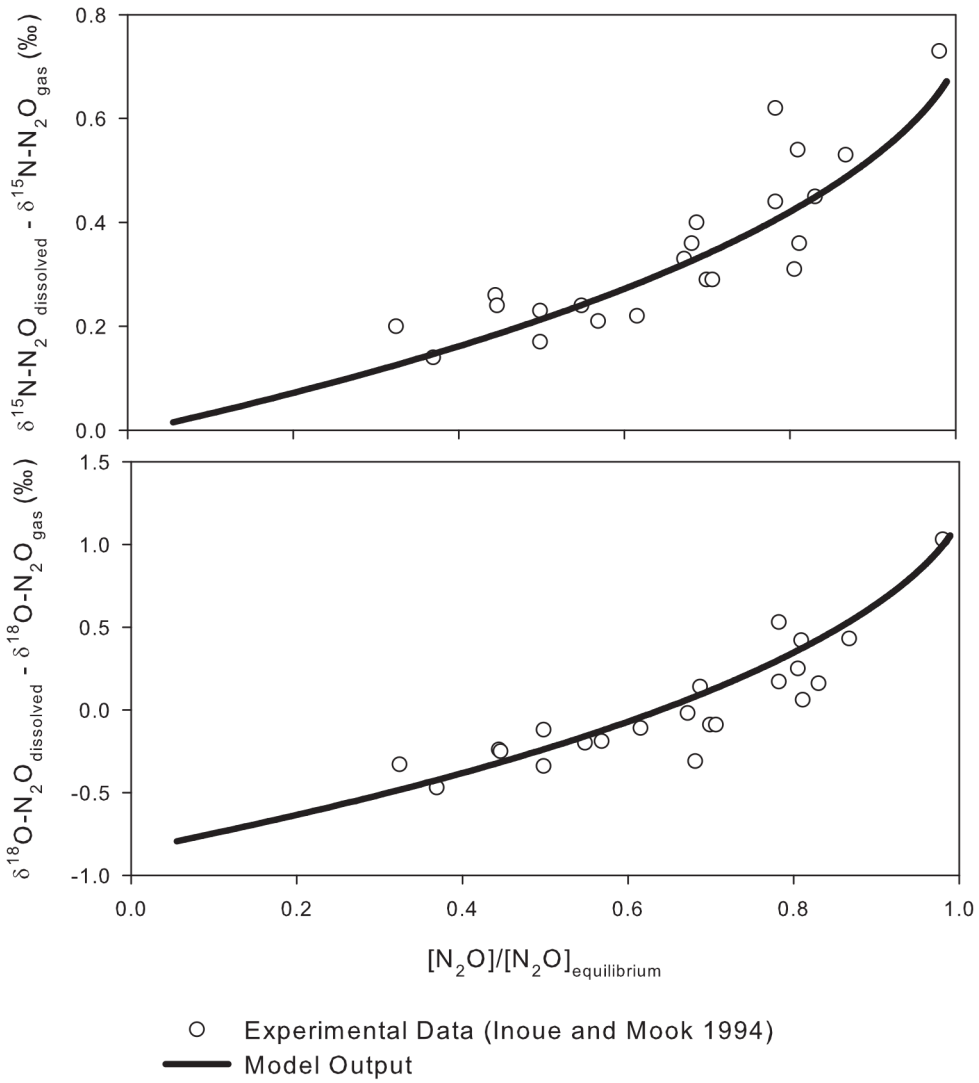

Figure 1. Comparing the model output to the experimental data of [22]. The coefficient of determination for experimental data and SIDNO model outputs were comparable to those of [22], $R^2 = 0.77$ for $\delta^{15}N$ and $R^2 = 0.82$ for $\delta^{18}O$. Precision of measurements for the experimental data was $\pm$ 0.05‰ for $\delta^{15}N$ and $\pm$ 0.1‰ for $\delta^{18}O$.
doi:10.1371/journal.pone.0090641.g001

Modelled dissolved N_2O concentration and δ values increased in response to gas exchange (Figure 1). The model fit to the experimental data is comparable to the original best-fit derivations ($R^2 = 0.77$ for $\delta^{15}N$ and $R^2 = 0.82$ for $\delta^{18}O$ for both the original fit [22] and the SIDNO fit) (Figure 1). The initial isotopic composition of dissolved N_2O was identical to the gas phase $\delta^{15}N$ value, but the $\delta^{18}O$ of dissolved N_2O was slightly less than the gas phase $\delta^{18}O$ value. Ultimately, at 100% saturation the δ values of the dissolved N_2O were greater than those of the gas phase as a result of α_{eq}. The model successfully simulated the kinetic and equilibrium fractionations during gas exchange under the experimental conditions.

Next, SIDNO was used to provide insight into the effect of degassing on the δ values of dissolved and emitted N_2O. Here the results of two model runs with the same initial N_2O concentration but different initial δ values of dissolved N_2O were compared (Figure 2). As N_2O saturation declined both the dissolved $\delta^{15}N$ values and instantaneous $\delta^{15}N$ values of the emitted N_2O remained relatively constant, dissolved $\delta^{18}O$ values and instantaneous $\delta^{18}O$ values of the emitted N_2O varied by about 10, when the solution was very supersaturated (>300% saturation). The δ values rose quickly as the system approached 100% saturation. Because the light isotopologue diffuses out of solution faster than the heavy isotopologue, the instantaneous δ values of the emitted N_2O were always less than the concomitant δ values of dissolved N_2O. The isotopologues of N_2O reached equilibrium independently of each other and therefore the total mass emitted for each isotopologue and rate of change depended on the initial concentration and δ values. The retention of N_2O in the dissolved phase caused the δ values of the mass emitted to differ from those of total mass production. However, when initial dissolved N_2O concentrations were high (>1000% saturation) the δ values of the total N_2O emitted were similar to the δ values of dissolved N_2O because the mass of N_2O lost is very much larger than the N_2O that remained dissolved. The value of k did not affect the gas exchange trajectories only the speed at which the system reached equilibrium.

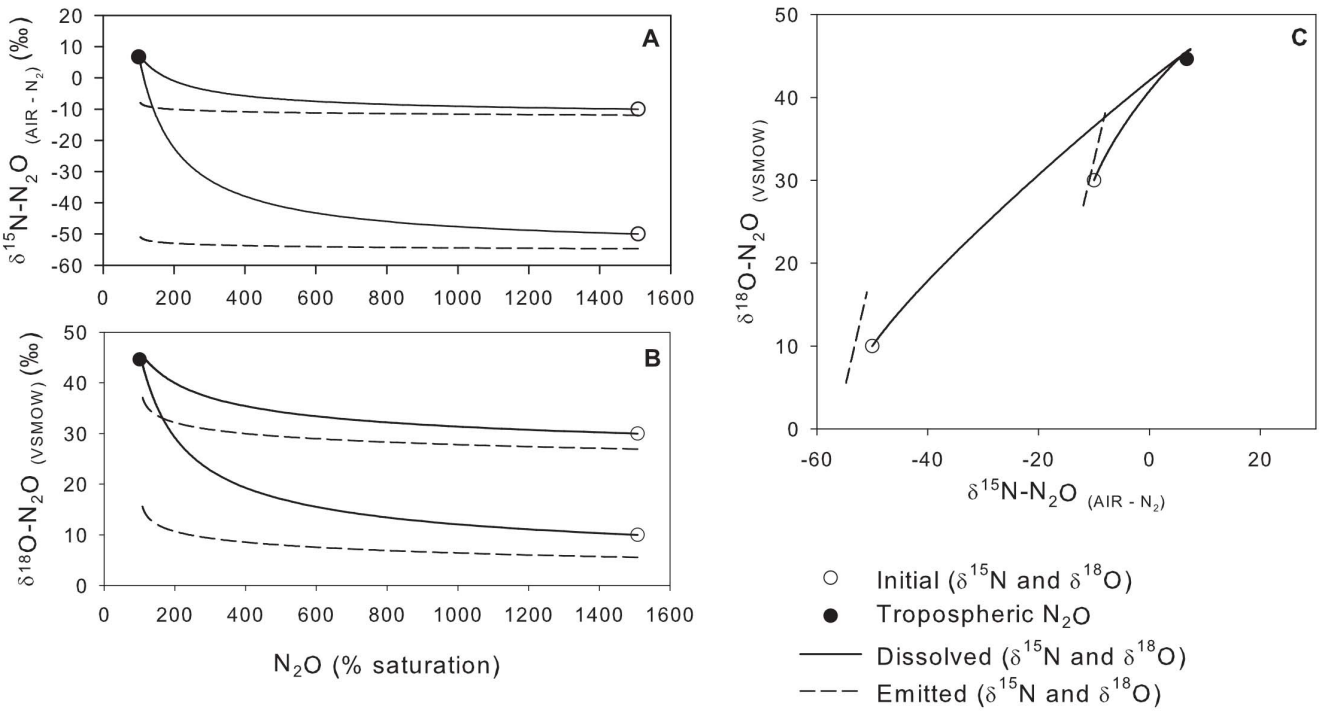

Figure 2. $\delta^{15}N$ and $\delta^{18}O$ trajectories for dissolved and emitted N_2O in two supersaturated solutions with zero N_2O production. Initial dissolved isotopic values for the two dissolved N_2O solutions were $\delta^{15}N = -50‰$, $\delta^{18}O = 10‰$, and $\delta^{15}N = -10‰$, $\delta^{18}O = 30‰$. Both runs used an initial dissolved N_2O concentration of 1500% saturation. Note that in the $\delta^{18}O$ versus $\delta^{15}N$ plot, the dissolved N_2O curves do not pass through the tropospheric N_2O value due to the small equilibrium isotope effect.
doi:10.1371/journal.pone.0090641.g002

N_2O isotope data are often plotted as $\delta^{18}O$ versus $\delta^{15}N$ to elucidate relationships between the various sources and tropospheric N_2O [38]. The trajectories on these plots (Figure 2C) were dictated by the δ values of the source relative to the constant atmospheric value and the α values. Note that some plots in the literature differ due to different reference materials for the $\delta^{18}O$ scale (VSMOW and atmospheric O_2).

Modelling Scenarios with Steady State Production of N_2O

The SIDNO model can be used to probe the stable isotope dynamics of N_2O in a variety of situations that may be encountered in aquatic environments to elucidate the relationship between the N_2O source (a function of N cycling processes), dissolved (the easily measured component), and emitted (of consequence for greenhouse gas production and global N and N_2O cycle).

In the steady-state production of N_2O (constant rate and δ values), by definition, the δ values of N_2O production must be the same as those of the emitted N_2O. As a result, the δ values of the dissolved N_2O cannot equal that of the source (or emitted) N_2O at steady state because the dissolved N_2O must be offset from the emitted N_2O by at least the α_{ev} values. As the steady-state production rate was increased, the steady-state N_2O concentration increased and the dissolved δ values approached but did not equal the source (Figure 3). Even at moderate supersaturations ($<1000\%$) the effect of atmospheric N_2O equilibration on the δ values of dissolved N_2O cannot be ignored.

At steady state, the δ values of the emitted N_2O must be equal to the source; the large difference between source/emitted and dissolved N_2O underscores the importance of adjusting the measured δ values of dissolved N_2O in order to determine aquatic contributions of N_2O to the atmosphere or N_2O sources. This is critical when using dissolved measurements of N_2O to constrain the global isotopic N_2O budget, but not been done in most studies, e.g., [16,42–44] but see [45].

Modelling Scenarios with Variable Production of N_2O

The relationship between the δ values of source, dissolved, and emitted N_2O are much more complicated when N_2O production is variable rather than when it is constant. N_2O production may vary with respect to production rate and/or δ values; in many aquatic environments, N_2O production is not likely to be constant. The N_2O production processes, nitrification and denitrification, are sensitive to redox conditions, which can be highly variable, due to diel changes in dissolved O_2 concentration, flow regime, etc. For example, [34] observed diel changes in the denitrification rate in the Iroquois River and Sugar Creek (Midwestern USA) and found that the denitrification was consistently greater during the day than night. The relative importance of nitrification and denitrification can change in response to the diel oxygen cycle: e.g., [46] observed a change from daytime nitrification to nighttime denitrification in a subtropical eutrophic stream. Coupling of N_2O and O_2 diel cycles has been observed in agricultural and waste-water treatment plant (WWTP) impacted rivers [36]. Since fractionation factors and substrates are different for nitrification and denitrification, ecosystem-scale fractionation factors may be rate and process dependent, and the δ values of N_2O production in a given ecosystem may not be constant over a diel cycle.

To simulate the diel variability, various scenarios were modelled by adjusting either production rate and/or the associated δ values. The variabilities in these input parameters were driven by a sine function with a 24 h period similar to a dissolve O_2 curve. In all scenarios, the chosen range of production rates was based on published N_2O flux rates (Table 1) and varied from 1 to

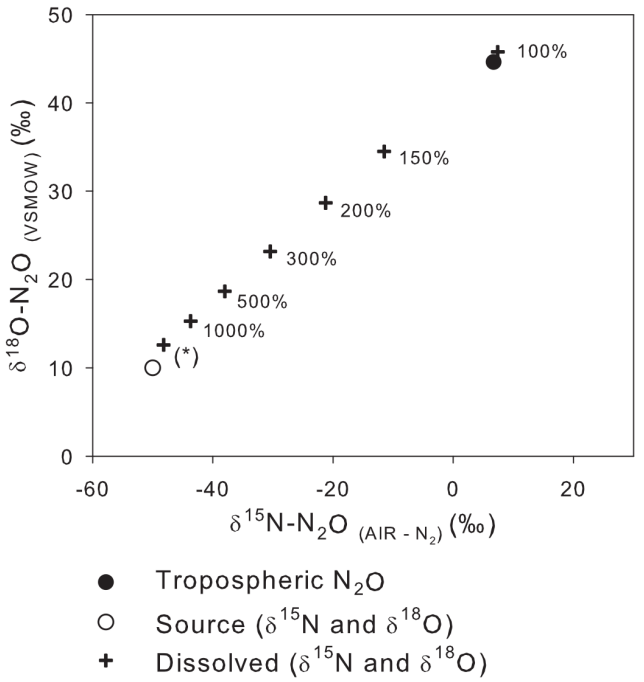

Figure 3. The relationship between $\delta^{15}N$, $\delta^{18}O$ and N_2O concentration in a system at steady state with constant N_2O production and open to gas exchange with the atmosphere. The point marked with a $*$ represents the minimum difference between the isotopic composition of dissolved and source N_2O. The point at 100% saturation is the equilibrium value, the $\delta^{15}N$ and $\delta^{18}O$ of this point is controlled by the isotopic composition of tropospheric N_2O and the equilibrium enrichment factors.
doi:10.1371/journal.pone.0090641.g003

5 mol/m^2/h^1 (Table 2), which was between the diel variation in N_2O flux observed by [33] and [46]. Temperature was held constant at 20°C. The value of k was varied between 0.1 and 0.3 m/d (Table 2), within the range observed in other river studies (Table 1). The combination of production rates and k values were chosen to produce N_2O between 150% and 500% saturation (Table 2) coinciding with the range of published data (Table 1). The range of δ values used for the N_2O source (Table 2) was within published values from various field studies [47]. For scenarios where the δ values of source N_2O was variable, the sine function for the δ values was synchronized so that maxima and minima $\delta^{15}N$ values coincided with those of $\delta^{18}O$. This was done for simplicity, and because, in general, nitrification yields N_2O with lower $\delta^{15}N$ and $\delta^{18}O$ values than denitrification (e.g., [10,48]). Nevertheless, scenarios with greater amounts of N_2O reduction to N_2 can be modelled by increasing the source $\delta^{15}N$ and $\delta^{18}O$ values to those appropriate for any given ecosystem. Model scenarios were run until the output parameters (i.e., N_2O saturation and the δ values of dissolved, source, and emitted N_2O) reached dynamic steady state: model output was not constant over 24 h but the diel patterns on successive days were repeated.

Model Scenario #1: Variable Production Rate, Constant Isotopic Composition of Source

In scenario #1 (Table 2), the δ values of source N_2O were held constant and the production rate was variable. An example of such a system may be N_2O production via denitrification in river sediments with abundant NO_3^-. Denitrification rates in rivers have been observed to fluctuate in response to the diel O_2 cycle [34]. If the fractionation factors for denitrification are not rate dependent, the resulting N_2O production rate would be variable but the source δ values of N_2O values could be constant.

Here, the maximum concentration lagged approximately 2.75 h behind the maximum N_2O production rate, a function of the magnitude of the gas exchange coefficient, cf. [49]. The δ values for the instantaneously emitted N_2O were relatively constant and very similar to the N_2O source (within 0.4‰ for $\delta^{15}N$ and 1.1‰ for $\delta^{18}O$, Figure 4, Table 3). However, the δ values of dissolved N_2O were more variable, spanning 16‰ for $\delta^{15}N$ and 10‰ for $\delta^{18}O$. Thus, a change in the δ values of dissolved N_2O can be driven simply by a change in production rate and not necessarily a change in the δ values of the source. Since the system was at dynamic steady state, the average δ values of the emitted N_2O were identical to the average δ values of the source. This must be true in all steady-state cases to conserve the mass of the N_2O isotopologues.

In some aquatic systems, the N_2O production rate may remain constant with time but the δ values of the source may change with time. In rivers or lakes without a strong diel O_2 cycle, sediment denitrification may produce N_2O at an approximately constant rate. Denitrification rate may also be independent of water column NO_3^- concentration if limited by factors other than diffusion in the sediments. The δ values of the source N_2O may thus change if the

Table 1. Summary of relevant published data on N_2O production in aquatic environments.

Location	Range of N_2O Saturation (%)	Range of N_2O Flux (μmol/m^2/h^1)	Range of k values (m/h)	Reference
Ohio River, OH, US	95 to 745	5 to 90	—	[12]
5 agricultural streams, ON, CA (over 2–3 years)	14 to 1700	−1 to 91.7	0.002 to 0.59	[5]
10 agricultural streams, ON, CA (over 17 diel cycles)	30 to 2570	−0.33 to 52.1	0.004 to 0.30	[45]
Bang Nara River, TH	170 to 2000	—	—	[20]
LII River, NZ	201 to 404	1.35 to 17.9	0.13 to 0.82	[58]
LII River, NZ	402 to 644	0.46 to 0.89	14.76	[33]
Seine River, FR	—	2.2 to 5.2	0.04 to 0.06	[59]
Canal Two, Yaqui Valley, MX	100 to 6000	0 to 34.9	0.3 to 0.6	[46]
agricultural stream, UK	100 to 630	0 to 37.5	—	[60]
Grand River, ON, CA	38 to 8573	−1.4 to 173.6	0.06 to 0.35	[36,37]

doi:10.1371/journal.pone.0090641.t001

Table 2. Summary of input parameters for the SIDNO model scenarios for non-steady state production of N_2O.

Scenario #	Results Figure	k	N_2O Source Production Rate	N_2O Source $\delta^{15}N$ and $\delta^{18}O$ Values
		(m/k)	(μmol/m^2/h^1)	(‰)
Variable Production Rate, Constant Isotopic Composition of Source				
1	4	0.3	1 to 5	−50, 10
Constant Production Rate, Variable Isotopic Composition of Source				
2	5	0.3	3	−50, 10 to −30, 10
3	6	0.1	3	−50, 10 to −30, 10
Variable Production Rate, Variable Isotopic Composition of Source				
4*	7	0.3	1 to 5	−50, 10 to −30, 10
5**	8	0.3	1 to 5	−50, 10 to −30, 10
6*	9	0.1	1 to 5	−50, 10 to −30, 10

*Maximum production rate coincides with the lowest source δ values.
**Maximum production rate coincides with the highest source δ values.
doi:10.1371/journal.pone.0090641.t002

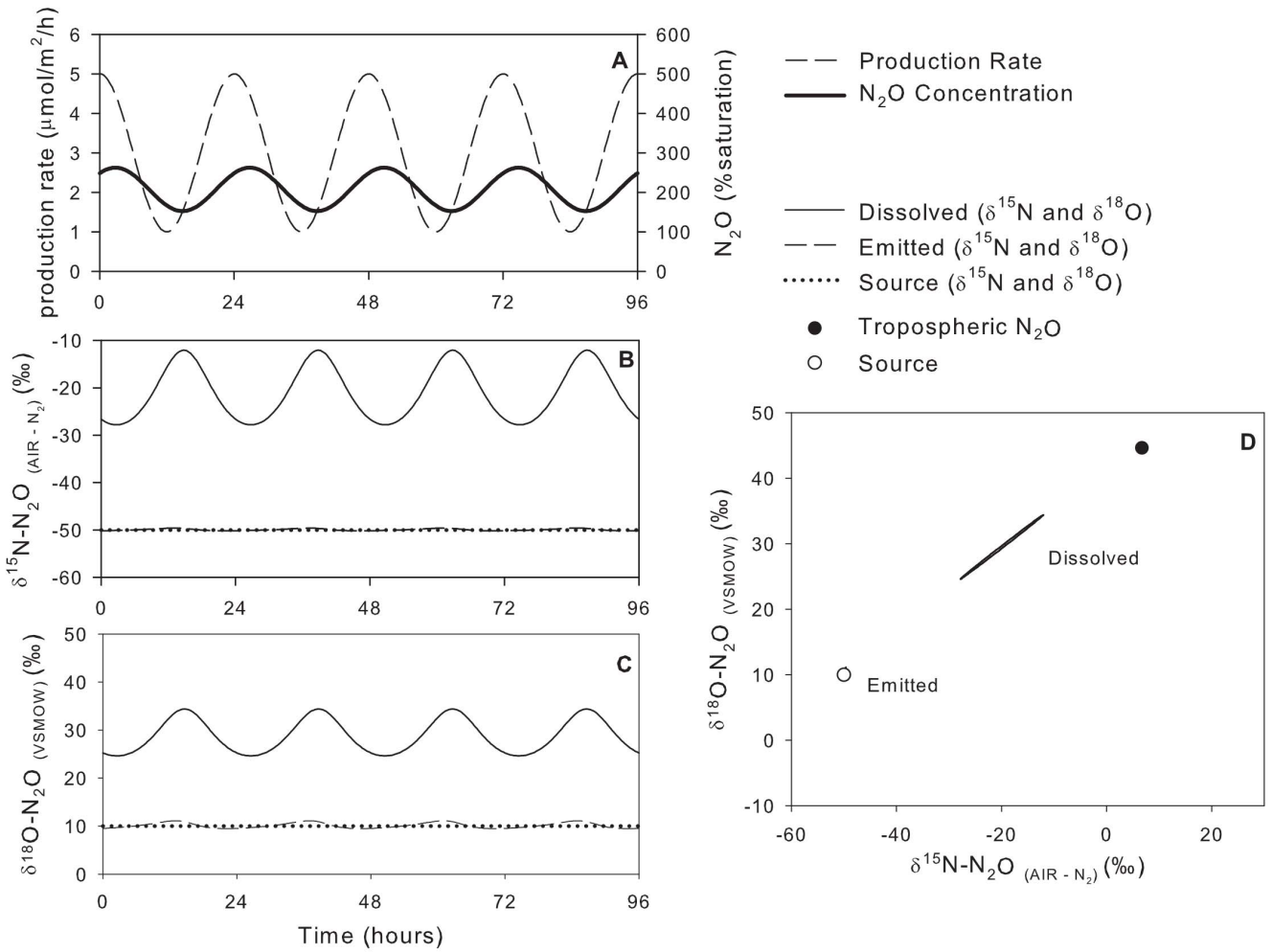

Figure 4. Model scenario #1 – isotopic composition of dissolved and emitted N_2O with a variable production rate and constant isotopic composition of the source. Note, in panel D, the data points for emitted N_2O are masked by the data point for source N_2O.
doi:10.1371/journal.pone.0090641.g004

Table 3. Summary of SIDNO output for model scenarios simulating non-steady state production of N_2O.

	Dissolved N_2O				Emitted N_2O		
Scenario #	Saturation	$\delta^{15}N$, $\delta^{18}O$	$\Delta\delta^{15}N$	$\Delta\delta^{18}O$	$\delta^{15}N$, $\delta^{18}O$	$\Delta\delta^{15}N$	$\Delta\delta^{18}O$
	(%)	(‰)	(‰)	(‰)	(‰)	(‰)	(‰)
Variable Production Rate, Constant Isotopic Composition of Source							
1	153 to 263	−27.8, 24.6 to −12.1, 34.4	37.9	24.4	−49.6, 9.5 to −50.2, 11.1	0.2	0.5
Constant Production Rate, Variable Isotopic Composition of Source							
2	208	−19.6, 29.4 to −3.7, to 37.4	30.4	19.4	−45.3, 12.3 to −14.7, 27.7	4.7	2.3
3	423	−26.1, 24.8 to −15.1, 30.3	23.9	14.8	−37.2, 16.4 to −22.8, 23.6	12.8	6.4
Variable Production Rate, Variable Isotopic Composition of Source							
4*	153 to 263	−25.8, 25.6 to −1.2, 39.8	24.2	15.6	−46.9, 11.3 to −18.0, 26.5	8	3.5
5**	153 to 263	−11.2, 33.8 to −5.0, 36.1	38.8	23.8	−41.6, 14.6 to −13.4, 28.1	8.4	4.6
6*	345 to 501	−31.6, 21.6 to −18.4, 29.3	18.4	11.6	−42.1, 13.7 to −29.4, 20.6	19.4	9.4

Temporally variable parameters are given as a range. $\Delta\delta^{15}N$ and $\Delta\delta^{18}O$ ($\Delta = \delta - \delta$) are the maximum difference between the range of source N_2O and the range for the model output parameter.
*Maximum production rate coincides with the lowest source δ values.
**Maximum production rate coincides with the highest source δ values.
doi:10.1371/journal.pone.0090641.t003

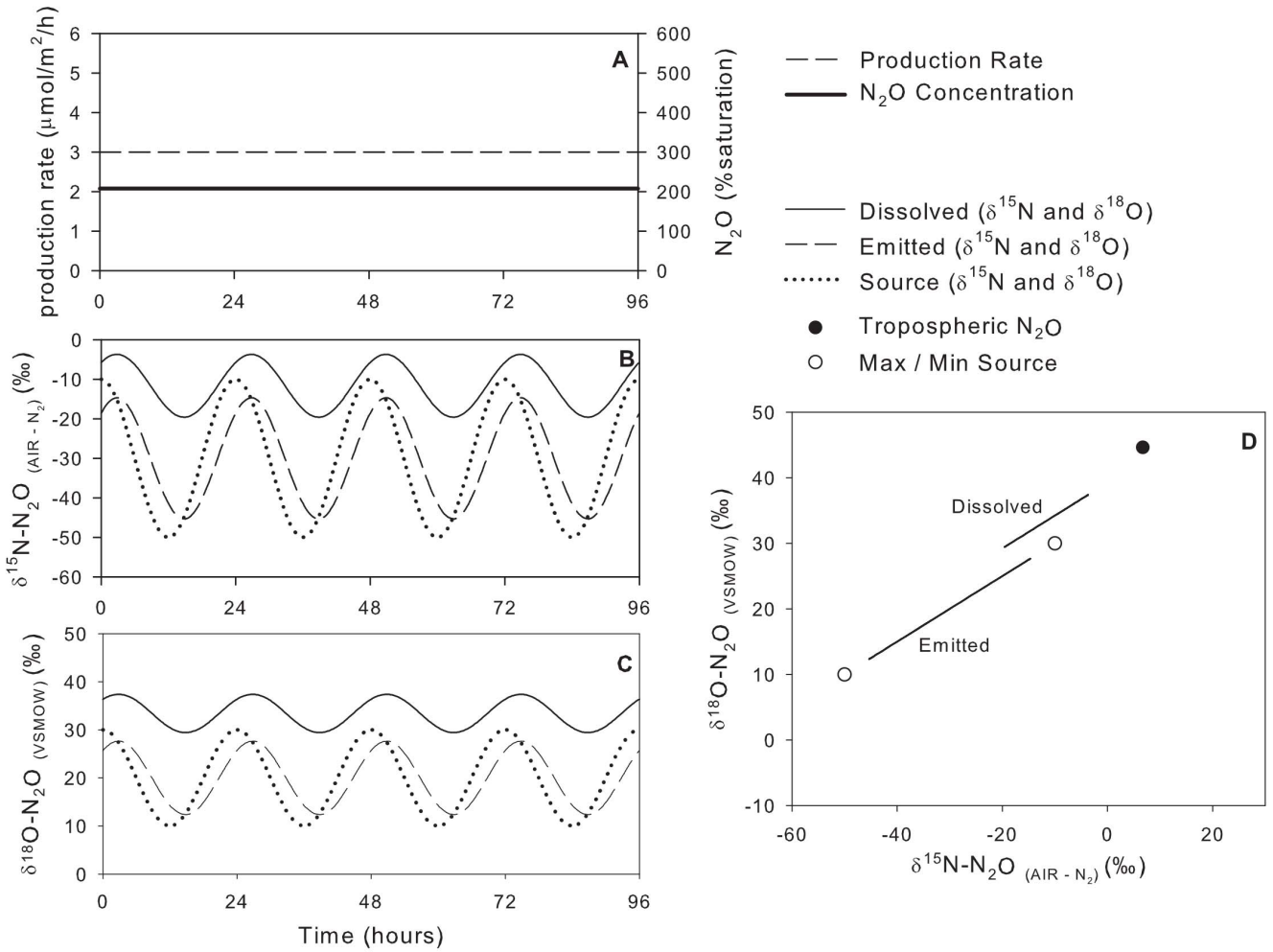

Figure 5. Model scenario #2 – Isotopic composition of dissolved and emitted with a constant production rate and variable isotopic composition of the source.
doi:10.1371/journal.pone.0090641.g005

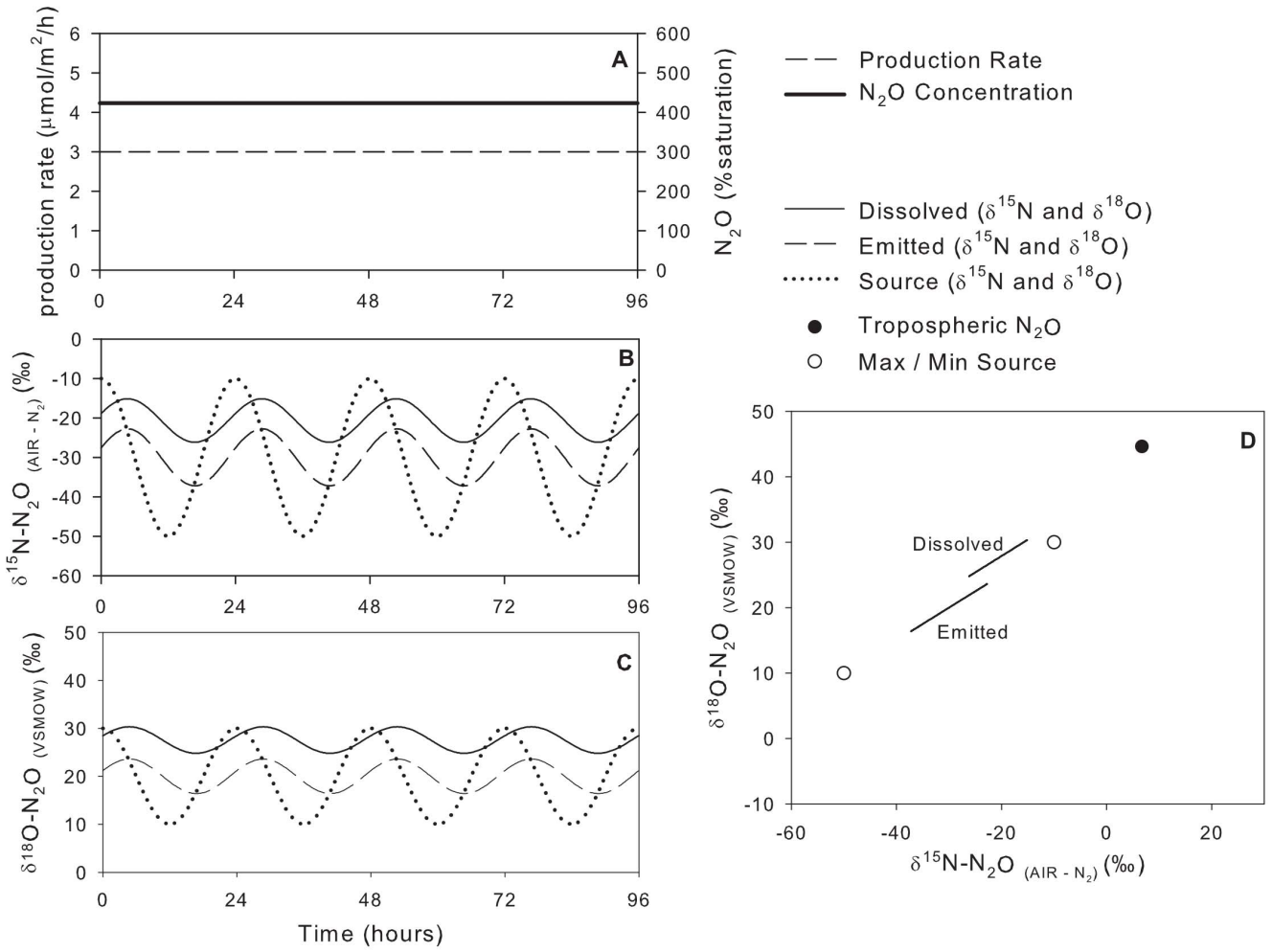

Figure 6. Model scenario #3 – Isotopic composition of dissolved and emitted N_2O with a constant production rate and variable isotopic composition of the source. k is reduced from 0.3 m/h to 0.1 m/h.
doi:10.1371/journal.pone.0090641.g006

δ values of the NO_3^- substrate changed with time. For example, many studies have shown that the δ values of residual NO_3^- increase during denitrification [50]. Similarly, NO_3^- from WWTPs may have different δ values than agricultural runoff and diel changes in WWTP release may result in changing δ values of NO_3^-. Changes in N cycling may also vary on a diel basis but result in fortuitously similar N_2O production rates due to, for example, changes in the N_2O:N_2 ratio of denitrification or changes in the relative importance of nitrification and denitrification. Thus changes in δ values of the N_2O source do not necessarily indicate changes in N_2O production rates.

Model Scenario #2: Constant Production Rate, Variable Isotopic Composition of Source

In scenario #2, when the N_2O production rate was held constant and the δ values of the source varied with time (from −50‰ to −10‰ for $\delta^{15}N$ and from 10‰ to 30‰ for $\delta^{18}O$), the δ values of the dissolved N_2O was also much farther from that of the source than the dissolved N_2O due to the effects of atmospheric exchange and the emitted N_2O varies linearly between the two source values. In contrast, the dissolved N_2O is parallel but offset from the line connecting the two sources (Figure 5, Table 3). The maximum difference between emitted and source N_2O was 4.7‰ for $\delta^{15}N$ and 2.3‰ for $\delta^{18}O$. The dissolved and emitted δ values also lagged 2.75 h behind the source as a result of gas exchange (as above). Since the system was at dynamic steady state, the average δ values of the emitted N_2O were identical to the average δ values of the source.

Model Scenario #3: Constant Production Rate, Variable Isotopic Composition of Source

To examine the effects of varying k on the scenario of constant N_2O production with variable isotopic signature of the source, k was reduced from 0.3 m/h (scenario #2) to 0.1 m/h (scenario #3; Figure 6, Table 3). The δ values for the emitted N_2O were centred between the sources N_2O values, but dissolved N_2O δ values were farther from tropospheric N_2O than the high-k scenario #2 (Figure 6 D).

The effect of reducing k was an increase in N_2O concentration with the same production rate and a shift in the δ values of dissolved N_2O toward the source values. Reducing k also dampened the response between the instantaneous δ values of the emitted N_2O and the δ values of the source. As above, the lag time between the δ values of the source and emitted N_2O increased as k decreased. The total range of the source and

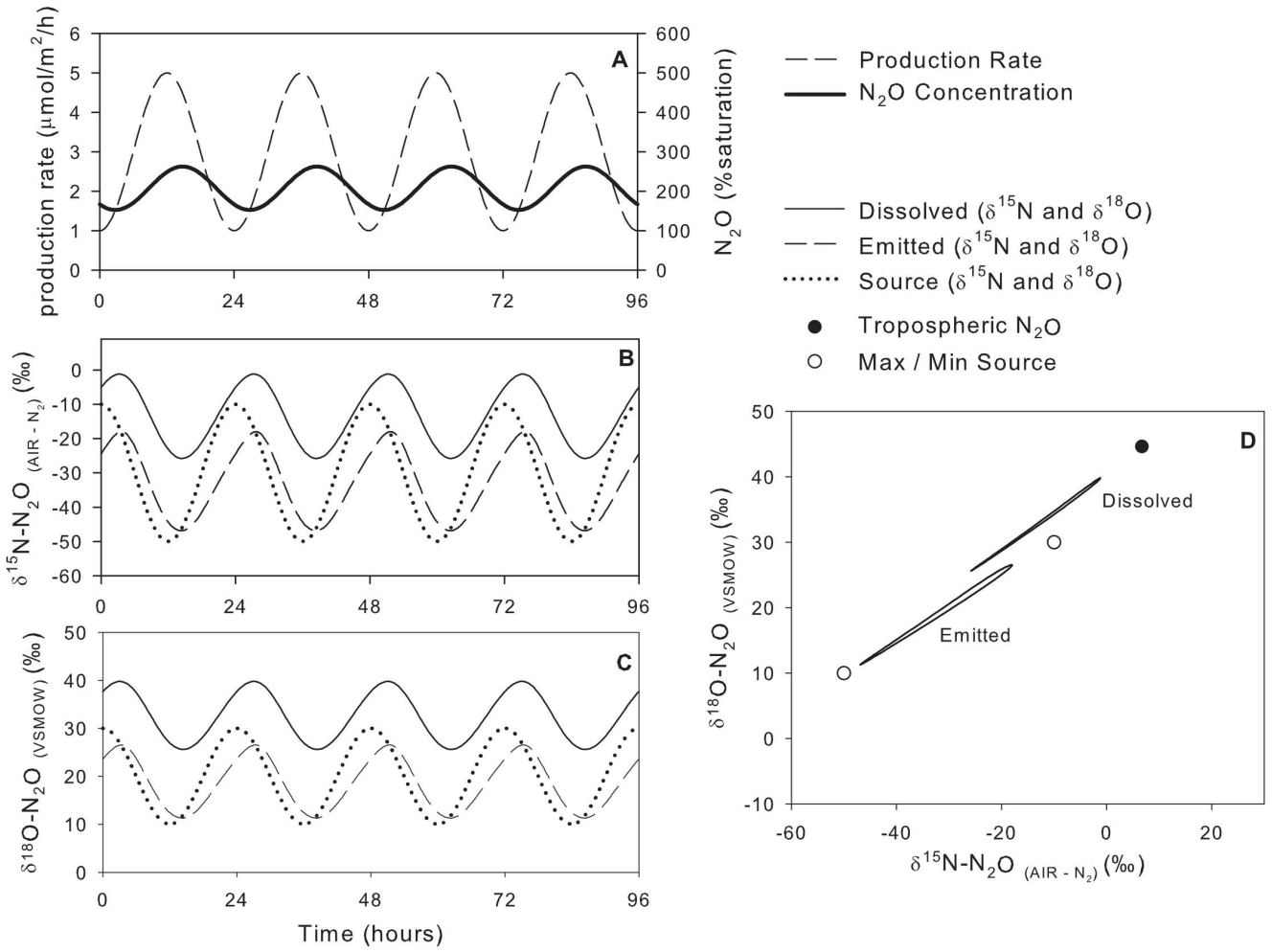

Figure 7. Model scenario #4 – Isotopic composition of dissolved and emitted N_2O with a variable production rate and variable isotopic composition of the source. Maximum production rate is in sync with the lowest $\delta^{15}N$ and $\delta^{18}O$ values of the source.
doi:10.1371/journal.pone.0090641.g007

emitted δ values decreased. The difference between the source and emitted δ values was 12.8‰ for $\delta^{15}N$ and 6.4‰ for $\delta^{18}O$.

To simulate a system alternating between two N_2O production processes, such as differing relative contributions of nitrification and denitrification, with different rates of N_2O production and δ values, the model was run with both production rate and its δ values variable with time (scenarios #4, #5, and #6). The production rate and δ values were adjusted so that the maximum rate coincided with the lowest source δ values in scenarios #4 and #6 and so that maximum rate coincided with the highest source δ values in scenario #5.

Model Scenario #4: Variable Production Rate, Variable Isotopic Composition of Source

For scenario #4, the resulting N_2O concentrations were identical to those in model scenario #1, with the maximum concentration lagging approximately 2.75 h behind the maximum production rate (Figure 7, Table 3). The relationship between the δ values of the dissolved and emitted N_2O was more complex than in other scenarios. The lag time between the maximum source δ values and those of dissolved and emitted N_2O (when the production rate was minimum) was 3.75 h; however, the lag time between the minimum source δ values and those of the dissolved and emitted N_2O (when the production rate was maximum) was only 2.25 h. The difference between the emitted and source N_2O was 3.1‰ to 8.0‰ for $\delta^{15}N$ and 1.3‰ to 3.4‰ for $\delta^{18}O$. The δ values of emitted N_2O were closer to those of the source during periods of high production rates (and thus higher concentrations) than periods of low production rates. However, the flux-weighted average δ values of emitted N_2O were equal to the average production-weighted source δ values because the system was at dynamic steady state.

Model Scenario #5: Variable Production Rate, Variable Isotopic Composition of Source

The isotopic counterpoint to scenario #4 is adjusting the timing of maximum N_2O production to coincide with the highest δ values of production (scenario #5). All other parameters were the same as scenario #4 (Table 3). The resulting pattern for the δ values of dissolved N_2O was very different than scenario #4 (Figure 8, Table 3). While the dissolved N_2O concentrations were identical to the model scenario #4, the δ values of dissolved N_2O were nearly constant with time. The relationship between the δ values of emitted and source N_2O was similar to scenario #4, although the instantaneous difference in δ values were slightly greater. The δ values of the dissolved N_2O were greatly dampened by the fact

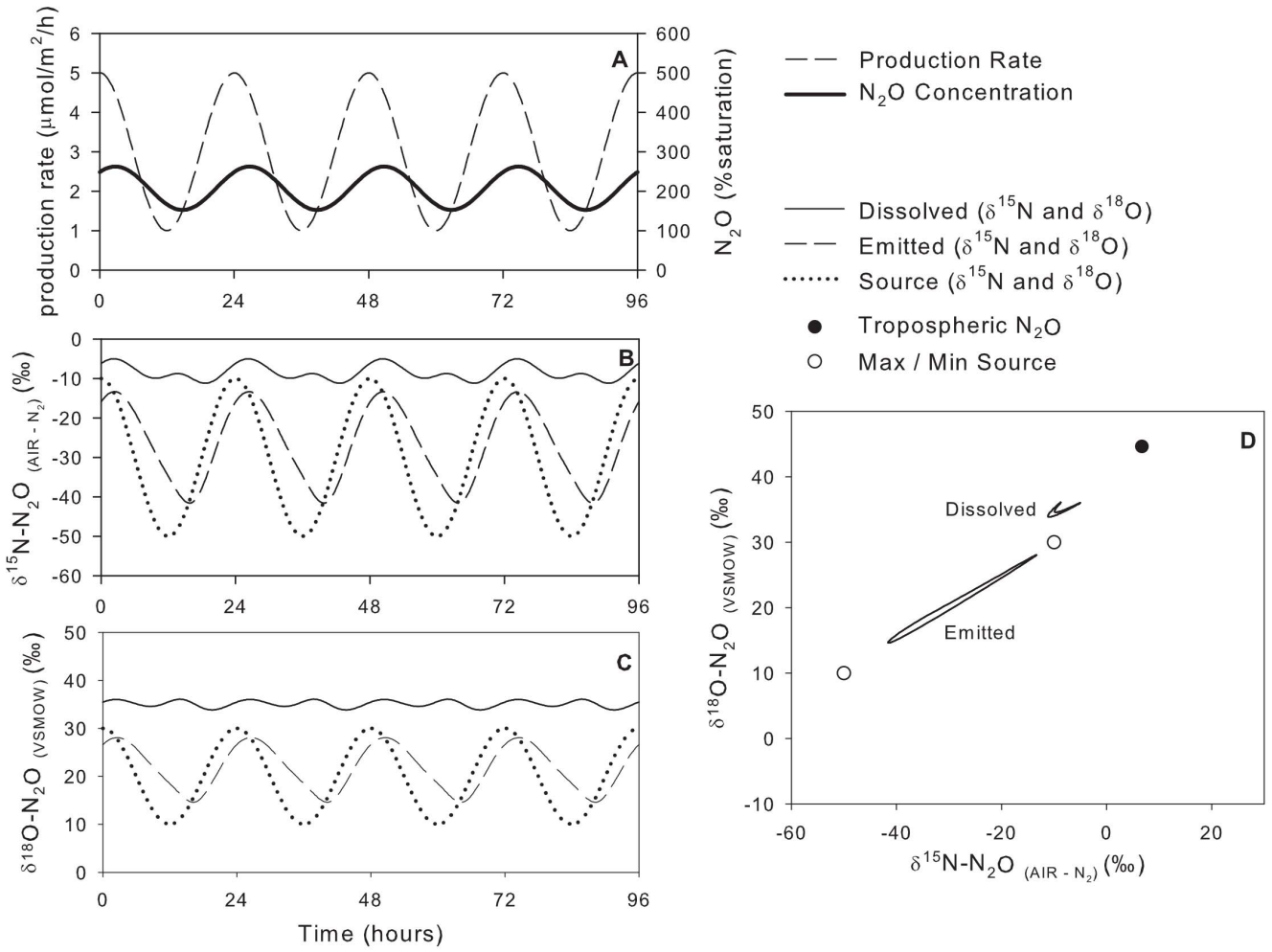

Figure 8. Model scenario #5 – Isotopic composition of dissolved and emitted N_2O with a variable production rate and variable isotopic composition of the source. Maximum production rate is in sync with the greatest $\delta^{15}N$ and $\delta^{18}O$ values of the source.
doi:10.1371/journal.pone.0090641.g008

that maximum production rate coincided with source δ values that were closest to tropospheric N_2O. In scenario #4, the high rates of N_2O production at δ values very different than tropospheric N_2O increased the amplitude of the δ values of dissolved N_2O.

Model Scenario #6: Variable Production Rate, Variable Isotopic Composition of Source

To determine the effects of a lower k on model scenario #4, k was reduced from 0.3 m/h from 0.1 m/h for scenario #6. As shown above, lower k increased the dissolved N_2O concentrations and dampened the diel range of δ values of both dissolved and emitted N_2O (Table 3, Figure 9). Lower k also increased the lag time between the δ values of emitted and source N_2O and increased the difference between the δ values of emitted and source N_2O (Figure 9). As in all scenarios, the flux-weighted average δ values of emitted N_2O were equal to the average production-weighted source δ values.

Grand River

The ability of SIDNO to reproduce measured patterns of N_2O concentration and δ values in a human-impacted river was also assessed. The Grand River is a seventh-order, 300 km long river that drains 6800 km^2 in southern Ontario, Canada, into Lake Erie, see [36,37,51]. There are 30 WWTPs in the catchment and their cumulative impact can be observed via the increase in artificial sweeteners in the river [52].

Samples were collected approximately hourly for 28 h at two sites in the central, urbanized portion of the river: sites 9 and 11 in [51,52]. The upstream site, Bridgeport, is where the river enters the urban section of the river at the city of Waterloo and is immediately above that city's WWTP. Blair is 26.6 km downstream of Bridgeport and below the cities of Waterloo and Kitchener. It is also 5.5 km downstream of the Kitchener WWTP. Average river depth at both sites was 30 cm. Values of k were determined by best-fit modelling of diel O_2 and $\delta^{18}O$-O_2 values at the sites [36]. N_2O concentration analyses were performed on a Varian CP-3800 gas chromatograph with an electron capture detector and isotopic ratio analyses were performed on a GV TraceGas pre-concentrator coupled to a GV Isoprime isotope ratio mass spectrometer, see [5] for analytical details.

Data from upstream and downstream of large urban wastewater treatment plants on the Grand River show diel patterns in N_2O saturation and δ values (Figures 10 and 11). At the Bridgeport site, the diel patterns of N_2O saturation and $\delta^{15}N$ values were opposite of each other, that is, when N_2O saturation was highest around sunrise the $\delta^{15}N$ values were lowest and when

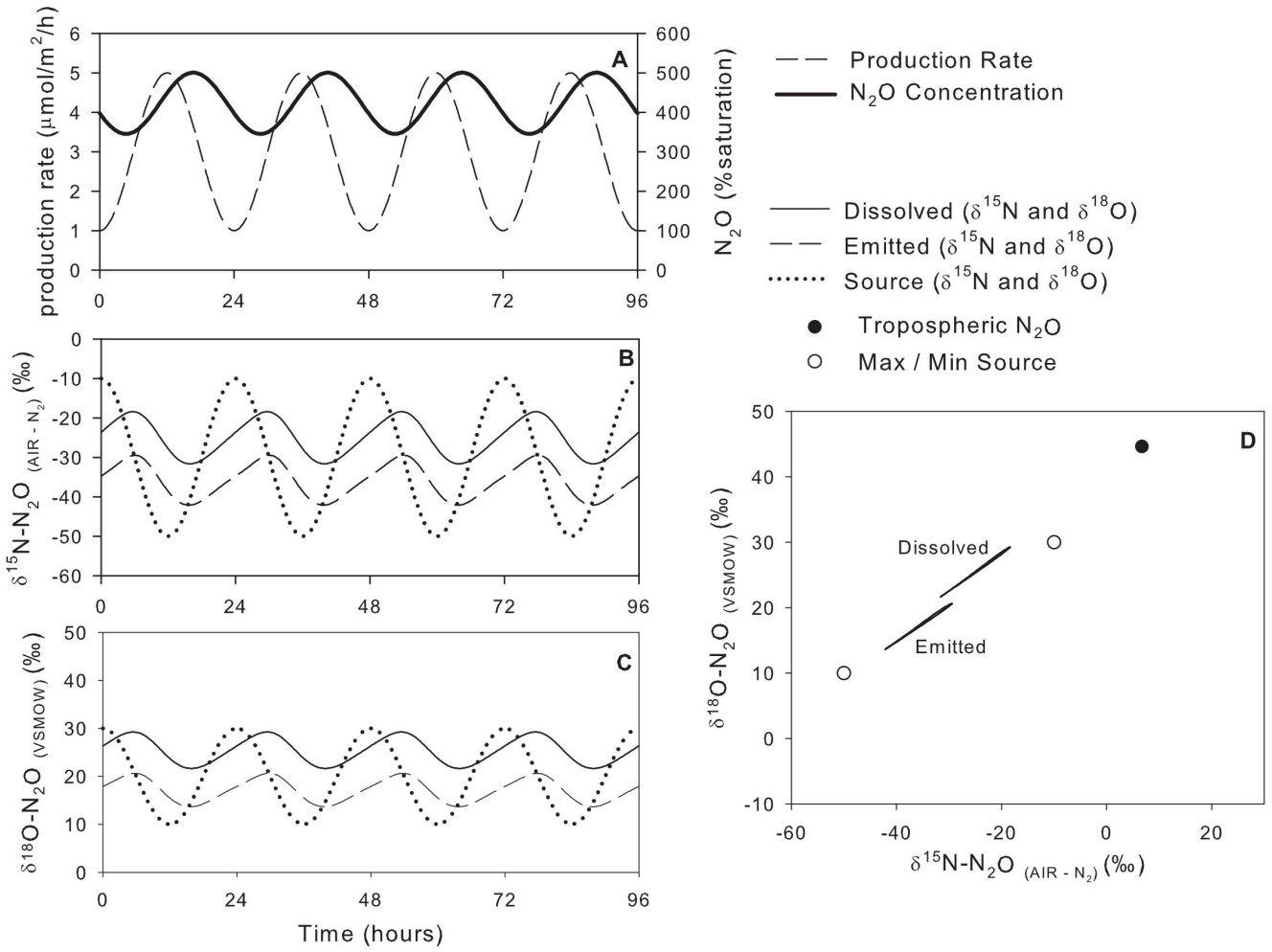

Figure 9. Model scenario #6 – Isotopic composition of dissolved N_2O and emitted N_2O with a variable production rate and variable isotopic composition of the source. Maximum production rate is in sync with the lowest $\delta^{15}N$ and $\delta^{18}O$ values of the source. k is reduced from 0.3 m/h to 0.1 m/h.
doi:10.1371/journal.pone.0090641.g009

when N_2O saturation was lowest around before sunset the $\delta^{15}N$ values were greatest. R^2 values between field and model data for N_2O saturation, $\delta^{15}N$, and $\delta^{18}O$ values are 0.83, 0.68, and 0.30. Model results reproduce the range and sinusoidal patterns of the field data though the $\delta^{18}O$ fit was poor in the second half of the field data. The diel pattern in $\delta^{18}O$ values was similar to that of $\delta^{15}N$ but was shifted earlier by about 4 h. These patterns were similar to those of scenario #4 (variable N_2O production and variable δ values of the source N_2O coinciding when maximum production rates coincided with lowest source δ values) and the result of consistent diel five-fold variability in N_2O production and variability in the $\delta^{18}O$ of the N_2O produced in the river.

At the downstream Blair site, both $\delta^{15}N$ and $\delta^{18}O$ values were much lower and exhibited a greater range than at Bridgeport. R^2 values between field and model data for N_2O saturation, $\delta^{15}N$, and $\delta^{18}O$ values are 0.78, 0.53, and 0.03. Model results reproduce the range and peak-and-trough pattern of the N_2O saturation and $\delta^{15}N$ data. Model results reproduce the range of $\delta^{18}O$ values but the pattern is not well reproduced. While all data at Bridgeport exhibited smooth, sinusoidal diel changes, the data at Blair show rapid changes. The diel patterns of N_2O saturation and $\delta^{15}N$ values were opposite of each other, that is, when N_2O saturation was highest around midnight, the $\delta^{15}N$ values were lowest and when when N_2O saturation was lowest during mid-day, the $\delta^{15}N$ values were greatest. The diel pattern in $\delta^{18}O$ values was more complex at Blair than at Bridgeport suggesting that daytime and nighttime were associated with different $\delta^{18}O$ values of N_2O production. These patterns were similar to those of scenario #5 (variable N_2O production and variable δ values of the source N_2O coinciding when maximum production rates coincided with highest source δ values) and the result of a five-fold variability in day-to-night N_2O production and variability in $\delta^{15}N$ and $\delta^{18}O$ of the N_2O produced in the river.

For both Bridgeport and Blair data, the cause of poorer fits for $\delta^{18}O$ than $\delta^{15}N$ deserve further research. Adding concomitant measurements of $\delta^{15}N$ and $\delta^{18}O$ values of NO_3^- may provide clues about N cycling and help explain some of the observed variability in N_2O [53]. Predicting $\delta^{18}O$-N_2O values from nitrification [11] and denitrification [54] is difficult because of the complex relationship between $\delta^{18}O$-H_2O values and $\delta^{18}O$-N_2O values. Additionally, diel variability in N_2O reduction to N_2 [45,46], may also manifest itself in $\delta^{18}O$-N_2O values because of the strong O isotope fractionation factor during denitrification [55].

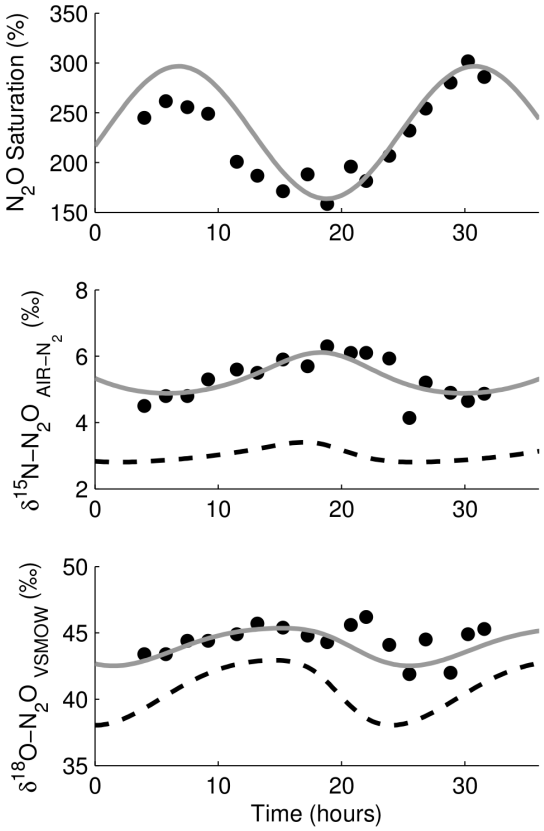

Figure 10. Diel variability in N_2O concentration and δ values at Bridgeport in the Grand River, Canada. The time axis begins at 00:00 on 2007-06-26. Maximum production rate is in sync with the greatest $\delta^{18}O$ values of the source, while $\delta^{15}N$ of the source was constant. R^2 values between field and model data for N_2O saturation, $\delta^{15}N$, and $\delta^{18}O$ values are 0.83, 0.68, and 0.30. This is similar to model scenario #4 (Figure 7).
doi:10.1371/journal.pone.0090641.g010

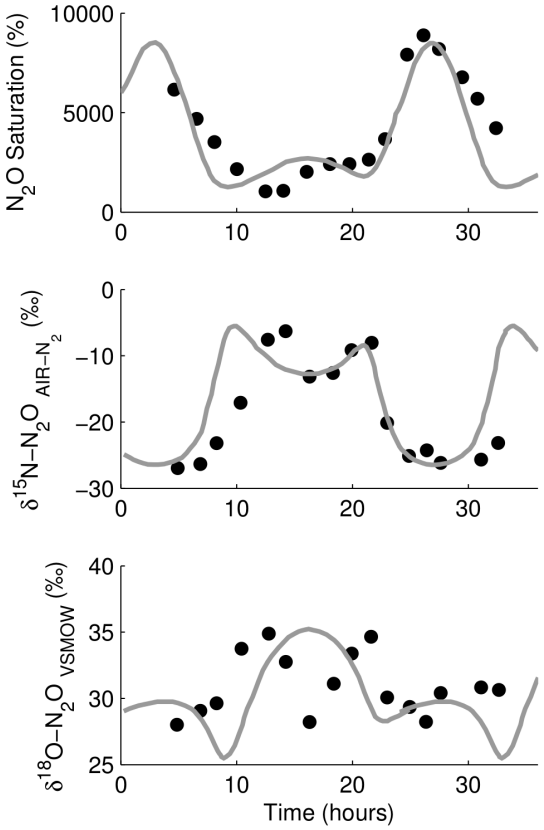

Figure 11. Diel variability in N_2O concentration and δ values at Blair in the Grand River, Canada. The time axis begins at 00:00 on 2007-06-26. Maximum production rate is in sync with the lowest $\delta^{15}N$ and $\delta^{18}O$ values of the source. R^2 values between field and model data for N_2O saturation, $\delta^{15}N$, and $\delta^{18}O$ values are 0.78, 0.53, and 0.03. This is similar to model scenario #5 (Figure 8).
doi:10.1371/journal.pone.0090641.g011

Discussion

Calculating the δ values of emitted or source N_2O is critical for regional and global N_2O isotopic budgets and also provides information about the source of N_2O and thus N cycling processes. However, SIDNO can simulate the relationships between the δ values of dissolved, source, and N_2O emitted from aquatic ecosystems to the atmosphere.In systems with N_2O production at dynamic steady state, the δ values of dissolved N_2O will not always be directly indicative of the δ values of the source N_2O. The difference between dissolved and source δ values increases as N_2O saturation decreases (as demonstrated in Figures 2 and 3). Even above 1000% saturation (from high production rates and/or low k), the δ values of dissolved N_2O will only approach δ values of the source but offset by 0.7‰ for $\delta^{15}N$ and 1.9‰ for $\delta^{18}O$, a result of the α_{ev} values (Figure 3). At constant N_2O production rates and δ values, the source and emitted δ values can be quantified since the δ values of emitted N_2O must be identical to those of the source and can be calculated from dissolved values (Figure 3; equations 5 and 6).

Our modelling results identified the limitations associated with simple interpretation of dissolved N_2O isotope data since the δ values of dissolved and emitted data are synchronous but rarely offset by a constant value. If N_2O saturation changes with time, the N_2O production rate must also have changed with time, provided k had been constant (compare model scenarios #1 and #2 in Figures 4 and 5). In contrast, changes in δ values of dissolved N_2O do not require a change in the source δ values (model scenario #1 and Figure 4), while constant δ values of dissolved N_2O do not require constant source δ values (for example model scenario #5 in Figure 8).

When δ values of the source N_2O are variable, the relationship between emitted and source N_2O becomes complicated. The δ values of emitted N_2O will lag behind those of the source and the amplitude of the diel range of δ values will be dampened relative to the source. The amount of lag and dampening is a function of k, N_2O production rate and timing, and the proximity of the source δ values to those of the atmosphere (compare Figures 2 with 3 and Figures 4 with 6). Qualitatively, the δ values of emitted N_2O will be similar to the source if the equilibration time of dissolved N_2O is small relative to the period of source variability (e.g., 24 h period due to diel changes in N cycling [36,45]). Assuming homogeneous N_2O release upstream, the equilibration time can be approximated from a decay curve as $\frac{3z}{k}$, where z is mean depth [49]. If z is small and/or k is high, the equilibration time will be short and the δ values of the emitted N_2O will be close to the source. With decreasing k (or increasing equilibration time), the δ values of emitted N_2O will lag farther behind and will always have a smaller range of δ values than the source. At the most extreme case, the variability in the δ values of emitted N_2O will be reduced to nearly

Table 4. Summary of the results of the SIDNO modelling as the predictive relationship between observations and implications.

Observed Parameter	Implications	Examples
Dissolved N_2O concentration is constant with time	The N_2O production rate is constant with time (if k and temperature are also constant). The N_2O flux to the atmosphere is equal to the production rate. This may not be true if the concentration is close to atmospheric equilibrium.	Scenarios #2 and #3
Dissolved N_2O concentration is variable with time in a sinusoidal pattern	The N_2O production rate is variable with time (if concentration change cannot be explained by change in k or temperature). The average N_2O flux to the atmosphere is equal to the average production rate.	Scenario #1
$\delta^{15}N$ and $\delta^{18}O$ of dissolved N_2O is constant with time	The observation is inconclusive. At concentrations near atmospheric equilibrium, isotopic composition of dissolved N_2O will approximate tropospheric N_2O, egardless of source values. A constant isotopic signature of dissolved N_2O that is different from tropospheric N_2O can indicate either a constant source (if production rate is constant), or a variable source.	Scenario #5
$\delta^{15}N$ and $\delta^{18}O$ of dissolved N_2O is variable with time (slope of data on a $\delta^{18}O$–$\delta^{15}N$ cross-plot tends toward tropospheric N_2O)	The change in $\delta^{15}N$ and $\delta^{18}O$ of dissolved N_2O is likely a result of a change in concentration, but it is possible that the source is variable with time, if the $\delta^{15}N$ and $\delta^{18}O$ values of the source also trend through the value for tropospheric N_2O.	Scenarios #1, #2, #4, and #6
Calculated $\delta^{15}N$ and $\delta^{18}O$ of emitted N_2O is constant with time	The isotopic composition of the source is constant with time, and equal to the calculated value for emitted N_2O	Scenario #1
Calculated $\delta^{15}N$ and $\delta^{18}O$ of emitted N_2O is variable with time	The isotopic composition of the source is variable with time. The range in $\delta^{15}N$ and $\delta^{18}O$ of emitted N_2O is the minimum for the range in that of the source. The flux weighted average $\delta^{15}N$ and $\delta^{18}O$ of emitted N_2O is equal to the production weighted average source values.	Scenarios #2–#6
Long residence time relative to variability of source (need to independently determine k)	The changes in N_2O concentration and $\delta^{15}N$ and $\delta^{18}O$ of emitted N_2O will be dampened relative to, and lag behind, that of the source	Scenarios #3 and #6
Short residence time relative to variability of source (need to independently determine k)	The changes in N_2O concentration and $\delta^{15}N$ and $\delta^{18}O$ of emitted N_2O will be indicative of changes in the source	Scenarios #1, #2, #3 and #4

doi:10.1371/journal.pone.0090641.t004

zero and δ values of the emitted N_2O would be equal to the average production-weighted source δ values. At very long equilibration times, the probability of N_2O consumption increases, a process not explicitly included in SIDNO where the δ value of the source N_2O is simply that which is released to the water column.

Separating N_2O production into nitrification and denitrification requires independent knowledge about the δ values of the source N and O in aquatic ecosystems. It is therefore not possible to state a single $\delta^{15}N$ value for nitrification–N_2O and one for denitrification–N_2O applicable to all aquatic ecosystems. The $\delta^{15}N$ value of the N_2O precursors NH_4^+ and NO_3^- vary across ecosystem as a result of human impact and N loading (agricultural and WWTP) as well as the source of N, and additional N transformations in the aquatic ecosystem. For example, along the length of the Grand River, $\delta^{15}N$ values of NH_4^+ and NO_3^- exhibit systematic trends resulting from the confluence of agricultural tributaries and large urban waste-water treatment plants (Schiff et al., unpublished results, [53]). Nevertheless, these values can be measured and biogeochemical relationships between N species, redox, and N_2O can be used as supporting information for process separation (e.g., [5,12,36,45]). The $\delta^{18}O$ value of N_2O will also vary across ecosystems as a result of its close relationship with $\delta^{18}O$-H_2O and to a lesser extent $\delta^{18}O$-O_2 [10,11,54,56]. Fortunately, $\delta^{18}O$-H_2O values can be easily predicted and measured [57]. Thus, once δ values of N_2O precursors have been identified, biogechemical data can provide an indication about the diel pattern of N_2O production processes, and ranges of potential end-member δ values can be calculated (e.g., [5] summarize isotopic fractionation for $\delta^{15}N$ and [10,11,54,56] for $\delta^{18}O$) and the model used to fit the field data.

Conclusions

In aquatic ecosystems, the instantaneous δ values of N_2O emitted to the atmosphere are easily calculated if the water temperature and dissolved N_2O concentration and δ values are known. Our modelling efforts illustrate that complex relationships exist between dissolved and source N_2O and that the δ values of dissolved N_2O are not always representative of either the N_2O produced or emitted to the atmosphere. Thus, calculated δ values of the emitted N_2O are the values that should be used to draw conclusions about N_2O emission from aquatic systems and the global N_2O cycle rather than the more commonly used instantaneous values (Table 4). The flux-weighted δ values of emitted N_2O can provide average production-weighted δ values of the N_2O source under dynamic steady-state in aquatic ecosystems.

If the δ values of emitted N_2O are constant with time, either the δ values of the source must also be constant or the N_2O equilibration time is very long. However, if the calculated δ values of emitted N_2O vary with time then the δ values of the source must also vary with time producing a diagnostic pattern. These findings are more robust than using dissolved δ values alone since dissolved

δ values can change simply with a change in N_2O production rate, changes in source δ values, and changes in k. N_2O residence time, dependent on production rate, k, and z, will determine the lag time between the δ values of emitted and source N_2O. The difference in timing between maxima and minima δ values of emitted N_2O and the maxima and minima of dissolved N_2O is indicative of how the δ values of the source change. For all these reasons, we urge caution when using single samples of N_2O concentration and δ to calculate fluxes of N_2O to the atmosphere and inferring N_2O production pathways.

Ultimately, the dynamic model SIDNO may be used to estimate k, N_2O production rate and δ values of the N_2O source, an indication of the production pathway and N cycling, in aquatic ecosystems via inverse modelling. If physical properties, such as depth and temperature are known, SIDNO may be used to fit the measured field data (N_2O concentration and δ values) by adjusting the N_2O source parameters. SIDNO can also be used to explore the dynamics between dissolved, source, and emitted N_2O to query production scenarios and design field campaigns for studies of N cycling processes.

Acknowledgments

We thank MS Rosamond, HM Baulch, the reviewers, and the academic editor for their helpful comments.

Author Contributions

Conceived and designed the experiments: SJT JJV SLS. Performed the experiments: SJT JJV. Analyzed the data: SJT JJV SLS. Contributed reagents/materials/analysis tools: SJT JJV SLS. Wrote the paper: JJV SJT SLS.

References

1. Forster P, Ramaswamy V, Artaxo P, Berntsen T, Betts R, et al. (2007) Changes in atmospheric constituents and in radiative forcing. In: Solomon S, Qin D, Manning M, Chen Z, Marquis M, et al., editors, Climate Change 2007: The Physical Science Basis. Contribution of Working Group I to the Fourth Assessment Report of the Intergovernmental Panel on Climate Change. Cambridge: Cambridge University Press.
2. Denman KL, Brasseur G, Chidthaisong A, Ciais P, Cox PM, et al. (2007) Couplings between changes in the climate system and biogeochemistry. In: Solomon S, Qin D, Manning M, Chen Z, Marquis M, et al., editors, Climate Change 2007: The Physical Science Basis. Contribution of Working Group I to the Fourth Assessment Report of the Intergovernmental Panel on Climate Change. Cambridge: Cambridge University Press.
3. Wada E, Ueda S (1996) Carbon nitrogen and oxygen isotope ratios of CH_4 and N_2O on soil ecosystems. In: Boutton TW, Yamasaki SI, editors.Mass Spectrometry of Soils.New York: Marcel Dekker. pp. 177–204.
4. Aravena R, Mayer B (2010) Isotopes and processes in the nitrogen and sulfur cycles. In: Environmental isotopes in biodegradation and bioremediation. Boca Raton, FL: Lewis Publishers. pp. 203–246.
5. Baulch HM, Schiff SL, Thuss SJ, Dillon PJ (2011) Isotopic character of nitrous oxide emitted from streams. Environ Sci Technol 45: 4682–4688.
6. Park S, Pérez T, Boering KA, Trumbore SE, Gil J, et al. (2011) Can N_2O stable isotopes and isotopomers be useful tools to characterize sources and microbial pathways of N_2O production and consumption in tropical soils? Global Biogeochem Cycles 25: GB1001.
7. Bol R, Toyoda S, Yamulki S, Hawkins JMB, Cardenas LM, et al. (2003) Dual isotope and isotopomer ratios of N_2O emitted from a temperate grassland soil after fertiliser application. Rapid Commun Mass Spectrom 17: 2550–2556.
8. Mandernack KW, Rahn T, Kinney C, Wahlen M (2000) The biogeochemical controls of the $\delta^{15}N$ and $\delta^{18}O$ of N_2O produced in landfill cover soils. J Geophys Res Atmos 105: 17709–17720.
9. Pérez T, Trumbore SE, Tyler SC, Matson PA, Ortiz-Monasterio I, et al. (2001) Identifying the agricultural imprint on the global N_2O budget using stable isotopes. J Geophys Res Atmos 106: 9869–9878.
10. Snider DM, Schiff SL, Spoelstra J (2009) ^{15}N /^{14}N and ^{18}O/^{16}O stable isotope ratios of nitrous oxide produced during denitrification in temperate forest soils. Geochim Cosmochim Acta 73: 877–888.
11. Snider DM, Venkiteswaran JJ, Schiff SL, Spoelstra J (2012) Deciphering the oxygen isotope composition of nitrous oxide produced by nitrification. Glob Chang Biol 18: 356–370.
12. Beaulieu JJ, Shuster WD, Rebholz JA (2010) Nitrous oxide emissions from a large, impounded river: The Ohio River. Environ Sci Technol 44: 7527–7533.
13. Beaulieu JJ, Tank JL, Hamilton SK, Wollheim WM, Hall RO Jr, et al. (2011) Nitrous oxide emission from denitrification in stream and river networks. Proc Natl Acad Sci USA 108: 214–219.
14. Dore JE, Popp BN, Karl DM, Sansone FJ (1998) A large source of atmospheric nitrous oxide from subtropical north pacific surface waters. Nature 396: 63–66.
15. Kim KR, Craig H (1990) Two-isotope characterization of N_2O in the Pacific Ocean and constraints on its origin in deep water. Nature 347: 58–61.
16. Naqvi S, Yoshinari T, Jayakumar D, Altabet M, Narvekar P, et al. (1998) Budgetary and biogeochemical implications of N_2O isotope signatures in the Arabian Sea. Nature 394: 462–464.
17. Priscu JC, Christner BC, Dore JE, Westley MB, Popp BN, et al. (2008) Supersaturated N_2O in a perenniallyice-covered Antarctic lake: Molecular and stable isotopic evidence for a biogeochemical relict. Limnol Oceanogr 53: 2439–2450.
18. Yoshinari T, Altabet M, Naqvi S, Codispoti L, Jayakumar A, et al. (1997) Nitrogen and oxygen isotopic composition of N_2O from suboxic waters of the eastern tropical north pacific and the arabian sea–measurement by continuous-ow isotope-ratio monitoring. Mar Chem 56: 253–264.
19. Kroeze C, Dumont E, Seitzinger SP (2005) New estimates of global emissions of N_2O from rivers and estuaries. Environ Sci 2: 159–165.
20. Boontanon N, Ueda S, Kanatharana P, Wada E (2000) Intramolecular stable isotope ratios of N_2O in the tropical swamp forest in Thailand. Naturwissenschaften 87: 188–192.
21. Toyoda S, Iwai H, Koba K, Yoshida N (2009) Isotopomeric analysis of N_2O dissolved in a river in the tokyo metropolitan area. Rapid Commun Mass Spectrom 23: 809–821.
22. Inoue HY, Mook WG (1994) Equilibrium and kinetic nitrogen and oxygen isotope fractionations between dissolved and gaseous N_2O. ChemGeol 113: 135–148.
23. Brenninkmeijer CAM, Rckmann T (1999) Mass spectrometry of the intramolecular nitrogen isotope distribution of environmental nitrous oxide using fragmention analysis. Rapid Commun Mass Spectrom 13: 2028–2033.
24. Sutka RL, Ostrom N, Ostrom P, Breznak J, Gandhi H, et al. (2006) Distinguishing nitrous oxide production from nitrification and denitrification on the basis of isotopomer abundances. Appl Environ Microbiol 72: 638–644.
25. Toyoda S, Yoshida N (1999) Determination of nitrogen isotopomers of nitrous oxide on a modified isotope ratio mass spectrometer. Anal Chem 71: 4711–4718.
26. Röckmann T, Kaiser J, Brenninkmeijer CAM, Brand WA (2003) Gas chromatography/isotoperatio mass spectrometry method for high-precision position-dependent ^{15}N and ^{18}O measurements of atmospheric nitrous oxide. Rapid Commun Mass Spectrom 17: 1897–1908.
27. Venkiteswaran JJ, Wassenaar LI, Schiff SL (2007) Dynamics of dissolved oxygen isotopic ratios: a transient model to quantify primary production, community respiration, and air–water exchange in aquatic ecosystems. Oecologia 153: 385–398.
28. Wahlen M, Yoshinari T (1985) Oxygen isotope ratios in N_2O from different environments. Nature 313: 780–782.
29. Zafiriou OC (1990) Laughing gas from leaky pipes. Nature 347: 15–16.
30. Westley MB, Yamagishi H, Popp BN, Yoshida N (2006) Nitrous oxide cycling in the black sea inferred from stable isotope and isotopomer distributions. Deep Sea Res Part II 53: 1802–1816.
31. Well R, Eschenbach W, Flessa H, von der Heide C, Weymann D (2012) Are dual isotope and isotopomer ratios of N_2O useful indicators for N_2O turnover during denitrification in nitratecontaminated aquifers? Geochim Cosmochim Acta 90: 265–282.
32. An S, Joye SB (2001) Enhancement of coupled nitrification-denitrification by benthic photosynthesis in shallow estuarine sediments. Limnol Oceanogr 46: 62–74.
33. Clough TJ, Buckthought LE, Kelliher FM, Sherlock RR (2007) Diurnal uctuations of dissolved nitrous oxide (N_2O) concentrations and estimates of N_2O emissions from a spring-fed river: implications for IPCC methodology. Glob Chang Biol 13: 1016–1027.
34. Laursen AE, Seitzinger SP (2004) Diurnal patterns of denitrification, oxygen consumption and nitrous oxide production in rivers measured at the whole-reach scale. Freshwat Biol 49: 1448–1458.
35. Lorenzen J, Larsen LH, Kjr T, Revsbech NP (1998) Biosensor determination of the microscale distribution of nitrate, nitrate assimilation, nitrification, and denitrification in a diatom-inhabited freshwater sediment. Appl Environ Microbiol 64: 3264–3269.
36. Rosamond MS, Thuss SJ, Schiff SL (2011) Coupled cycles of dissolved oxygen and nitrous oxide in rivers along a trophic gradient in Southern Ontario, Canada. J Environ Qual 40: 256–270.
37. Rosamond MS, Thuss SJ, Schiff SL (2012) Dependence of riverine nitrous oxide emissions on dissolved oxygen levels. Nat Geosci 5: 715–718.
38. Kaiser J, Röckmann T, Brenninkmeijer CAM (2003) Complete and accurate mass spectrometric isotope analysis of tropospheric nitrous oxide. J Geophys Res Atmos 108: 4476.

39. Prinn R, Cunnold D, Rasmussen R, Simmonds P, Alyea F, et al. (1990) Atmospheric emissions and trends of nitrous oxide deduced from 10 years of ALE–GAGE data. J Geophys Res Atmos 95: 18369–18385.
40. Prinn RG, Weiss RF, Fraser PJ, Simmonds PG, Cunnold DM, et al. (2000) A history of chemically and radiatively important gases in air deduced from ALE/GAGE/AGAGE. J Geophys Res Atmos 105: 17751–17792.
41. Lide DR, Frederikse HPR (1995) CRC Handbook of Chemistry and Physics, 76th edition. Boca Raton: CRC Press.
42. McElroy MB, Jones DBA (1996) Evidence for an additional source of atmospheric N_2O. Global Biogeochem Cycles 10: 651–659.
43. Rahn T, Wahlen M (2000) A reassessment of the global isotopic budget of atmospheric nitrous oxide. Global Biogeochem Cycles 14: 537–543.
44. Stein LY, Yung YL (2003) Production, isotopic composition, and atmospheric fate of biologically produced nitrous oxide. Annu Rev Earth Planet Sci 31: 329–356.
45. Baulch HM, Dillon PJ, Maranger R, Venkiteswaran JJ, Wilson HF, et al. (2012) Night and day: short-term variation in nitrogen chemistry and nitrous oxide emissions from streams. Freshwat Biol 57: 509–525.
46. Harrison JA, Matson PA, Fendorf SE (2005) Effects of a diel oxygen cycle on nitrogen transformations and greenhouse gas emissions in a eutrophied subtropical stream. Aquat Sci 67: 308–315.
47. Rock L, Ellert BH, Mayer B, Norman AL (2007) Isotopic composition of tropospheric and soil N_2O from successive depths of agricultural plots with contrasting crops and nitrogen amendments. J Geophys Res Atmos 112: D18303.
48. Kool DM, Wrage N, Oenema O, Dolfifing J, Van Groenigen JW (2007) Oxygen exchange between (de)nitrification intermediates and H_2O and its implications for source determination of NO_3 and N_2O: a review. Rapid Commun Mass Spectrom 21: 356–3578.
49. Chapra SC, Di Toro DM (1991) Delta method for estimating primary production, respiration, and reaeration in streams. J Environ Eng 117: 640–655.
50. Mengis M, Schif SL, Harris M, English MC, Aravena R, et al. (1999) Multiple geochemical and isotopic approaches for assessing ground water no3 elimination in a riparian zone. Ground Water 37: 448–457.
51. Venkiteswaran JJ, Rosamond MS, Schiff SL (2014) Nonlinear response of riverine N_2O uxes to oxygen and temperature. Environ Sci Technol 48: 1566–1573.
52. Spoelstra J, Schiff SL, Brown SJ (2013) Artificial sweeteners in a large canadian river reect human consumption in the watershed. PLoS ONE 8: e82706.
53. Hood JLA, Taylor WD, Schiff SL (2013) Examining the fate of WWTP effluent nitrogen using $\delta^{15}N$ -NH_4^+, $\delta^{15}N$ -NO_3^-, and $\delta^{15}N$ of submersed macrophytes. Aquat Sci. doi: 10.1007/s00027-013-0333-4.
54. Snider DM, Venkiteswaran JJ, Schiff SL, Spoelstra J (2013) A new mechanistic model of $\delta^{18}O$-N_2O formation by denitrification. Geochim Cosmochim Acta 112: 102–115.
55. Well R, Flessa H (2009) Isotopologue enrichment factors of N_2O reduction in soils. Rapid Commun Mass Spectrom 23: 2996–3002.
56. Snider DM, Spoelstra J, Schiff SL, Venkiteswaran JJ (2010) Stable oxygen isotope ratios of nitrate produced from nitrification: ^{18}O-labeled water incubations of agricultural and temperate forest soils. Environ Sci Technol 44: 5358–5364.
57. Bowen GJ, Wassenaar LI, Hobson KA (2005) Global application of stable hydrogen and oxygen isotopes to wildlife forensics. Oecologia 143: 337–348.
58. Clough TJ, Bertram JE, Sherlock RR, Leonard RL, Nowicki BL (2006) Comparison of measured and ef5-r-derived N_2O uxes from a spring-fed river. Glob Chang Biol 12: 352–363.
59. Garnier J, Billen G, Cébron A (2007) Modelling nitrogen transformations in the lower Seine river and estuary (France): impact of wastewater release on oxygenation and N_2O emission. Hydrobiologia 588: 291–302.
60. Reay DS, Smith KA, Edwards AC (2003) Nitrous oxide emission from agricultural drainage waters. Glob Chang Biol 9: 195–203.